Engineering Quantum Jump Superoperators for Single Photon Detectors

A. V. Dodonov,[1,*] S. S. Mizrahi,[1,†] and V. V. Dodonov[2,‡]

[1] *Departamento de Física, CCET, Universidade Federal de São Carlos, Via Washington Luiz km 235, 13565-905, São Carlos, SP, Brazil*

[2] *Instituto de Física, Universidade de Brasília, PO Box 04455, 70910-900, Brasília, DF, Brazil*

(Dated: February 1, 2008)

We study the back-action of a single photon detector on the electromagnetic field upon a photodetection by considering a microscopic model in which the detector is constituted of a sensor and an amplification mechanism. Using the quantum trajectories approach we determine the Quantum Jump Superoperator (QJS) that describes the action of the detector on the field state immediately after the photocount. The resulting QJS consists of two parts: the bright counts term, representing the real photoabsorptions, and the dark counts term, representing the amplification of intrinsic excitations inside the detector. First we compare our results for the counting rates to experimental data, showing a good agreement. Then we point out that by modifying the field frequency one can engineer the form of QJS, obtaining the QJS's proposed previously in an *ad hoc* manner.

PACS numbers: 03.65.Ta, 42.50.Lc, 03.65.Yz, 42.50.Ct, 85.60.Gz

I. INTRODUCTION

Single photon detectors (SPD) represent the ultimate sensitivity limit for quantum photodetectors, and many quantum optics and quantum information applications are based on its existence [1]. Nowadays, there are several available types of SPD's sensitive to different light wavelengths and with a varying range of quantum efficiencies [2, 3, 4, 5, 6, 7, 8, 9, 10, 11, 12]. Among many applications, SPD's are the main ingredient in the situations where one measures the electromagnetic field (EM) with few photons enclosed in a cavity, the photons being counted one by one. Theoretical treatment of such a scheme, known as *continuous photodetection model* (CPM), was proposed by Srinivas and Davies (SD) in 1981 [13] and did find many applications since then [14, 15, 16].

In SD scheme, in each infinitesimal time interval the photodetector has only two possible outcomes: either a single photon is detected ('click' of the detector), or it is not. In both cases the state of the field changes as time goes on: for a click, the field loses one photon and suffers a *Quantum Jump*; for no-click the field state modifies continuously and non-unitarily due to the monitoring of the detector [17, 18]. Thus, besides allowing determination of the statistical properties of the EM field through photocounts statistics, the detector also exerts a back-action on the field by which the outcome of the measurement modifies the cavity field state [19]. This phenomenon was widely used for different theoretical proposals, e.g. for changing the field statistics from sub-Poissonian to super-Poissonian [20], for controlling the entanglement between two field modes [15] or inducing spin squeezing in a cavity [16]. However, no experimental verification of the CPM has been made until now, though nowadays it is quite realistic to make simple photocounting experiments for testing the theory, provided one takes into account inevitable losses present in the experiment and include them into the model [21, 22].

Here we study how the field state after the click depends on detector's parameters. It is worth considering how SPD's actually operate: despite technical and structural differences associated with every kind of detector, the photodetection process is based on the same principle: the 'sensor' initially set in a 'ground state' interacts with the field and is likely to absorb a photon, doing a transition to the 'excited state'. After some time the sensor decays back to the ground state, emitting a photoelectron that triggers the 'amplification mechanism' (AM) of the SPD (e.g., by an avalanche process), producing a pulse of macroscopic electric current or voltage, that originates a registered click of the detector, representing one count. Besides, in real photodetectors there is a phenomenon called *dark counts*: photoelectrons originated due to the intrinsic excitations inside the AM, and not due to the absorption of one photon from the field. The influence of dark counts on the results of various experiments was considered in [23, 24, 25, 26, 27], and different schemes of calculating dark count probability and single-photon quantum efficiency were used in [28, 29, 30].

In the CPM, all the results concerning the photodetection process are described by means of a single entity characterizing the photodetector — the Quantum Jump Superoperator (QJS) $\hat{J}$, that represents the back-action of the detector on the field upon a single photodetection. Immediately after the photodetection an initial field state described by the statistical operator ρ changes abruptly to $\rho' = \hat{J}\rho/\mathrm{T}r[\hat{J}\rho]$, and the probability for registering one count during the time interval $[t, t+\Delta t)$ is $\mathrm{Tr}[\hat{J}\rho]\Delta t$, where Δt is the time resolution of the detector. It is supposed that Δt is small compared to other characteristic time scales and that QJS is time-independent, in an ideal

*Electronic address: adodonov@df.ufscar.br
†Electronic address: salomon@df.ufscar.br
‡Electronic address: vdodonov@fis.unb.br

case being given by

$$\hat{J}\rho \equiv \gamma_O \hat{O}\rho\hat{O}^{\dagger}, \tag{1}$$

where $\hat{O}$ is a lowering operator responsible for subtracting one photon from the field and γ_O is roughly the counting rate [18] with dimension (time^{-1}).

Srinivas and Davies proposed *ad hoc* $\hat{O} = \hat{a}$, where $\hat{a}$ is the bosonic lowering operator. In spite of having some inconsistencies as noted by the authors themselves, this QJS has been widely used since then. Recently, another QJS defined with $\hat{O} = \hat{E}_- \equiv (\hat{n}+1)^{-1/2}\,\hat{a}$ (where $\hat{n} \equiv \hat{a}^{\dagger}\hat{a}$) was proposed, also *ad hoc*, in [31, 32] – we named it 'E-model' for simplicity. The differences between these two QJS's were studied in [18], showing that the inconsistencies of the SD-model are indeed eliminated.

In [33] we have proposed a microscopic model (some other models were considered in [34, 35]) for the field-detector interaction, where we showed that both QJS's proposed *ad hoc* are particular cases that can be derived from a general time-dependent '*transition*' superoperator. However, there we considered a simplified model of the detector at 'zero temperature', by assuming that there were no intrinsic excitations inside the photodetector and that the sensor was at exact resonance with the field mode. Here we relax these conditions, being less stringent, we take into account the effects implied by a 'non-zero temperature' detector possessing intrinsic excitations and allow a detuning between the field and sensor frequencies. Moreover, we attribute numerical values for the model parameters in order to reproduce experimental data both qualitatively and quantitatively. We show that the dark counts appear naturally in our model, and comparing the predicted counting rates and Signal-to-Noise ratio with experimental data, we get a good qualitative and quantitative agreement. Furthermore, we demonstrate that the actual expression for the QJS should be incremented as (cf. Ref. [23])

$$\hat{J}\rho = \gamma_O \hat{O}\rho\hat{O}^{\dagger} + \gamma_D \hat{D}\rho\hat{D}^{\dagger}, \tag{2}$$

where γ_D is roughly the dark counts rate and the operator $\hat{D}$ describes the back-action of the detector on the field due to dark counts. Finally, we point out that by simply modifying the field frequency we are able to engineer the QJS, thus obtaining either the SD-model or E-model in specific regimes.

The paper is organized as follows. In Sec. II we model the sensor of the photodetector as a 2-level system, according to the well known Jaynes–Cummings model; taking into account the effects of the sensor–AM coupling, we obtain an explicit form of the transition superoperator, from which we derive a general expression for the QJS. In Sec. III we compare our results for counting rates with experimental data and obtain specific expressions of the QJS for different field wavelengths. The section IV contains the summary and conclusions.

II. MODELLING THE PHOTODETECTOR

We assume the SPD as being constituted of two parts: the sensor and the AM. The sensor is modelled as a two-level quantum object with resonant frequency ω_0, interacting with the mono-modal EM field with frequency ω (for multi-modal field one should just consider a frequencies distribution). It has a ground and an excited states $|g\rangle$ and $|e\rangle$ (before and after the photoabsorptions), so we describe it by the usual Jaynes–Cummings Hamiltonian [36] (for its applicability see, e.g. [37, 38] and references therein)

$$H_0 = \frac{1}{2}\omega_0\sigma_0 + \omega\hat{n} + g\hat{a}\sigma_+ + g^*\hat{a}^{\dagger}\sigma_-, \tag{3}$$

where g is the sensor-field coupling constant, and the sensor operators are $\sigma_0 = |e\rangle\langle e| - |g\rangle\langle g|$, $\sigma_+ = |e\rangle\langle g|$ and $\sigma_- = |g\rangle\langle e|$. We assume g being real, since only its absolute value enters the final expressions.

Upon absorbing a photon the sensor initially in the ground state jumps to the excited state and some time later it decays back emitting a photoelectron into the AM. The AM is a complex macroscopic structure that depends on the type of SPD; it amplifies the photoelectron and originates some observable macroscopic effect, giving rise to the clicks of the detector. In order to describe general features of the AM independent of the type of SPD, we model it as a thermal reservoir with a mean intrinsic excitations number $\bar{n}$. Thus, the whole system field–SPD is described by the effective 'standard master equation' [39]

$$\begin{aligned}\dot{\rho}_T &= \frac{1}{i}\left[H_0, \rho_T\right] - \gamma\overline{n}\left(\sigma_-\sigma_+\rho_T - 2\sigma_+\rho_T\sigma_- + \rho_T\sigma_-\sigma_+\right)\\ &- \gamma\left(\overline{n}+1\right)\left(\sigma_+\sigma_-\rho_T - 2\sigma_-\rho_T\sigma_+ + \rho_T\sigma_+\sigma_-\right),\end{aligned} \tag{4}$$

where γ is the sensor-AM coupling constant (we do not consider the field damping due to cavity losses).

According to CPM the trace of QJS gives the probability density p(t) for the photodetection, i.e. emission of a photoelectron at time t, given that at time $t = 0$ the detector-field system was in the state

$$\rho_0 = |g\rangle\langle g| \otimes \rho, \tag{5}$$

where the field state is ρ. Microscopically this means that in the time interval $(0, t)$ the sensor has undergone a transition $|g\rangle \to |e\rangle$ due to the absorption of one photon, and p(t)Δt is the probability for decaying back to the ground state during the time interval $[t, t+\Delta t)$, emitting a photoelectron that will lately originate one click. Following the quantum trajectories approach [39], p(t) is calculated from the master-equation (4) by identifying the sensor decay superoperator

$$\hat{R}\rho_0 = 2\gamma\left(\overline{n}+1\right)\sigma_-\rho_0\sigma_+ \tag{6}$$

describing the instantaneous $|e\rangle \to |g\rangle$ decay and the consequent emission of a photoelectron. The no-decay

superoperator $\hat{U}_t\rho_0 = \rho_U(t)$ describes the non-unitary evolution of the field–SPD system from $t = 0$ to $t > 0$ without emission of photoelectrons; $\rho_U(t)$ is the solution to the master equation (4) without the decay term (6):

$$\frac{d}{dt}\rho_U = -i(H_e\rho_U - \rho_U H_e^\dagger) + 2\gamma\overline{n}\sigma_+\rho_U\sigma_-, \quad (7)$$

where the effective non-Hermitian Hamiltonian is

$$H_e = \frac{(\omega_0 - i\gamma)}{2}\sigma_0 + \omega\hat{n} + g\hat{a}\sigma_+ + g\hat{a}^\dagger\sigma_- - i\gamma(\overline{n} + \frac{1}{2}). \quad (8)$$

Thus the probability density for the observation of a photocount, or a click, at time t is equal to

$$\mathrm{p}(t) = \mathrm{Tr}_{F-D}\left[\hat{R}\hat{U}_t\rho_0\right],$$

where $\hat{R}\hat{U}_t\rho_0$ represents an evolution of the field-SPD system from initial state ρ_0 at time $t = 0$ to the time t without any decay of the sensor and an instantaneous decay at the time t. Moreover, taking the trace only of the detector variables, one obtains the expression describing the action of the detector on the field upon the click – a predecessor of QJS that we call *transition superoperator*

$$\hat{\Xi}(t)\rho = \mathrm{Tr}_D\left[\hat{R}\hat{U}_t\rho_0\right], \quad (9)$$

from which the probability density for a count is $\mathrm{p(t)} = \mathrm{Tr}\left[\Xi(\mathrm{t})\rho\right]$.

Thus, for obtaining the transition superoperator one should first determine the no-decay superoperator $\hat{U}_t$ and then evaluate Eq. (9) using the initial state (5). In order to solve Eq. (7) we do the transformation

$$\rho_U = X_t\tilde{\rho}_U X_t^\dagger, \quad (10)$$

where

$$X_t = \exp(-iH_e t), \quad (11)$$

and obtain a simple equation for $\tilde{\rho}_U$

$$\frac{d}{dt}\tilde{\rho}_U = 2\gamma\overline{n}\widetilde{\sigma}_+\tilde{\rho}_U\widetilde{\sigma}_-, \quad (12)$$

$$\widetilde{\sigma}_+ = X_{-t}\sigma_+X_t, \qquad \widetilde{\sigma}_- = \widetilde{\sigma}_+^\dagger, \quad (13)$$

whose formal solution is

$$\tilde{\rho}_U(t) = \rho_0 + 2\gamma\overline{n}\int_0^t dt'\widetilde{\sigma}_+(t')\tilde{\rho}_U(t')\widetilde{\sigma}_-(t'). \quad (14)$$

Now one iterates Eq. (14) and obtains a power expansion in terms of $\bar{n}$, substitutes the result into Eq. (10) and then evaluates Eq. (9), finally obtaining

$$\hat{\Xi}(t)\rho = 2bg\left(1 + \bar{n}\right)\sum_{l=0}^{\infty}\left(2\gamma\bar{n}\right)^l\hat{\Xi}_l(t)\rho, \quad (15)$$

where for $l > 0$

$$\hat{\Xi}_l(t)\rho = \int_0^t dt_1\cdots\int_0^{t_{l-1}} dt_l\hat{\theta}_l\rho\hat{\theta}_l^\dagger \quad (16)$$

$$\hat{\theta}_l(t, t_1, \cdots, t_l) = \langle e|X_t\widetilde{\sigma}_+(t_1)\widetilde{\sigma}_+(t_2)\cdots\widetilde{\sigma}_+(t_l)|g\rangle. \quad (17)$$

For $l = 0$ the integrals and the terms $\widetilde{\sigma}_+$ should be dropped out:

$$\hat{\Xi}_0(t)\rho = \hat{\theta}_0\rho\hat{\theta}_0^\dagger, \quad \hat{\theta}_0(t) = \langle e|X_t|g\rangle. \quad (18)$$

After some algebraic manipulations [40, 41] we get for (11)

$$\begin{aligned} X_t &= \exp\left[-\gamma t\left(\overline{n} + 1/2\right) - i\omega\hat{n}t\right] \quad (19)\\ &\times \left\{\chi_{\hat{n}+1}(t)|e\rangle\langle e| + \chi_{\hat{n}}(-t)|g\rangle\langle g|\right.\\ &\left.-ie^{-i\omega t/2}S_{\hat{n}+1}(t)\hat{a}\sigma_+ - ie^{i\omega t/2}S_{\hat{n}}(t)\hat{a}^\dagger\sigma_-\right\}, \end{aligned}$$

where

$$C_{\hat{n}}(t) = \cos\left(\gamma t B_{\hat{n}}/b\right), \; S_{\hat{n}}(t) = \sin\left(\gamma t B_{\hat{n}}/b\right)/B_{\hat{n}}, \quad (20)$$

$$\chi_{\hat{n}} = e^{-i\omega t/2}\left[C_{\hat{n}}(t) - i\delta S_{\hat{n}}(t)\right], \quad (21)$$

$$B_{\hat{n}} = \sqrt{\hat{n} + \delta^2}, \quad (22)$$

$$\delta = (q - ib)/2, \quad q \equiv \left(\omega_0 - \omega\right)/g, \quad b \equiv \gamma/g. \quad (23)$$

As will be shown later, in realistic cases we need only the first three terms of the expansion (15), whose constituents are found to be

$$\begin{aligned} \hat{\theta}_0 &= -ie^{-\gamma t(\overline{n}+1/2)-i\omega(\hat{n}+1/2)t}S_{\hat{n}+1}(t)\hat{a} \quad (24)\\ \hat{\theta}_1 &= e^{-\gamma t(\overline{n}+1/2)-i\omega\hat{n}t}\chi_{\hat{n}+1}(t - t_1)\chi_{\hat{n}}(-t_1) \quad (25)\\ \hat{\theta}_2 &= -ie^{-\gamma t(\overline{n}+1/2)-i\omega(\hat{n}-1/2)t}\chi_{\hat{n}+1}(t - t_1) \quad (26)\\ &\times S_{\hat{n}}\left(t_1 - t_2\right)\chi_{\hat{n}-1}(-t_2)\hat{a}^\dagger. \end{aligned}$$

Substituting these expressions into Eqs. (15) - (18), the transition superoperator turns out to be time-dependent, contrary to the definition of a QJS. We proceed as in [33], defining the QJS as the time average of the transition superoperator over the time T (to be determined later) during which the photoelectron is emitted with high probability:

$$\hat{J}\rho \equiv \frac{1}{T}\int_0^T dt\;\hat{\Xi}(t)\rho. \quad (27)$$

Considering the weak coupling, $\omega, \omega_0 \gg \gamma, |g|$, under which both the Jaynes–Cummings Hamiltonian (3) and the master equation (4) are valid, and expressing the field density operator in Fock basis as

$$\rho = \sum_{m,n=0}^{\infty}\rho_{mn}|m\rangle\langle n|, \quad (28)$$

after the averaging in (27) the off-diagonal elements of $\hat{J}\rho$ vanish due to rapid oscillations of the terms $\exp(\pm i\omega t)$. This means that the photodetection destroys the coherence of the density matrix. This can be understood from the point of view of information theory: information flows from the field–sensor system to the AM, so decoherence is active; moreover, since counting photons informs only about diagonal elements, which are proportional to the number of photons, non-diagonal elements can be completely ignored. Therefore, from now on we shall treat only the diagonal elements of $\hat{J}\rho$ in (27). Applying the superoperators $\hat{\Xi}_l$ on the density matrix as in (15), after evaluating Eq. (27) one is left with

$$\hat{J}\rho \;=\; \sum_{n=0}^{\infty}\rho_{nn}\Big[nJ_n^{(B)}|n-1\rangle\langle n-1| + J_n^{(D)}|n\rangle\langle n| + (n+1)J_n^{(E)}|n+1\rangle\langle n+1| + \cdots\Big]. \tag{29}$$

After some lengthy however straightforward calculations one obtains the following expression for the first term in (29)

$$J_n^{(B)} = \frac{bg\,(1+\bar{n})}{\tau}\frac{F_n - G_n}{|B_n|^2}, \tag{30}$$

$$G_n \;=\; \frac{1}{(1+2\overline{n})^2+\phi_n^2}\Big\{1+2\overline{n}-\exp\left[-\tau(1+2\overline{n})\right] \times\;\left[(1+2\overline{n})\cos(\tau\phi_n)-\phi_n\sin(\tau\phi_n)\right]\Big\}, \tag{31}$$

$$F_n = \begin{cases} \dfrac{\tau}{2}+\dfrac{1-\exp\left[-2\tau(1+2\overline{n})\right]}{4(1+2\overline{n})}, & \text{if } \xi_n = \pm(1+2\overline{n}) \\ G_n\left(\phi_n \to i\xi_n\right), & \text{otherwise,} \end{cases} \tag{32}$$

$$\tau \equiv \gamma T, \qquad \phi_n \equiv \frac{2\mathrm{Re}\,(B_n)}{b}, \qquad \xi_n \equiv \frac{2\mathrm{Im}\,(B_n)}{b}. \tag{33}$$

Since expression (30) is too involved to be interpreted analytically, we shall treat it numerically, as well as ongoing terms. In order to evaluate them we expand the time-dependent functions (C_n and S_n, Eq. (20)) in terms of exponentials and integrate the resulting expressions, obtaining for the second term in (29) (here for complex B_n defined by Eq. (22))

$$J_n^{(D)} = \frac{g\bar{n}b^2\,(1+\bar{n})}{\tau}\sum_{j,k=1}^{4}\frac{W_jW_k^*}{y_j-y_k^*}\sum_{l=1}^{2}(-1)^l\,\frac{1-e^{i\alpha_l\tau}}{\alpha_l}, \tag{34}$$

where

$$\begin{aligned} \alpha_1 &= i(1+2\overline{n})+\left(\omega_j-\omega_k^*\right)/b, \\ \alpha_2 &= \alpha_1+\left(y_j-y_k^*\right)/b, \\ W_{1(2)} &= (1-\delta/B_{n+1})(1-(+)\delta/B_n), \\ W_{3(4)} &= W_{1(2)}\left(B_{n+1}\to -B_{n+1}\right), \\ w_1 &= w_2 = -w_3 = -w_4 = B_{n+1}, \\ y_1 &= -y_4 = -(B_{n+1}+B_n), \\ y_2 &= -y_3 = B_n - B_{n+1}. \end{aligned}$$

In the same manner one can obtain exactly all the further terms, but we shall not write the resulting expressions here.

The QJS (29) contains an infinite number of terms, so every time the detector emits a click, the field state ρ reduces to an incoherent mixture (due to the decoherence process described above) of different states, each one with its respective probability. Let us examine these terms more closely. The first term, with coefficient $J_n^{(B)}$, takes out a photon from the field and modifies the relative weight of the state components, so it represents a click preceded by a photoabsorption – we call this event a 'bright count'. The second term, dependent on $J_n^{(D)}$ and proportional to $\bar{n}$ (quite small as will be shown below), does not subtract photons from the field but only modifies the relative weight of the state components – it represents the dark count, when the detector emits a click due to the amplification of its intrinsic excitations. All further terms in Eq. (29) are proportional to $\bar{n}^l$, $l \geq 2$; they describe emissions of several photons into the field upon a click, so we call the first of these term $J_n^{(E)}$ the 'emission term'. We would like to stress again that all these processes happen simultaneously with different probabilities upon a click of the detector, so the post-measurement state of the field is a classical mixture of these events. We also note that there are many different phenomena that give rise to dark counts [5, 12, 28]; our model takes into account only those of them that cause the transition of the sensor from the ground to the excited state, and since the sensor state depends on the sensor-field interaction, the dark counts modify indirectly the relative weight between the field components, thus depending on n. The other physical phenomena that do not cause this transition should not in principle modify the relation between the field components and should be expressed by a constant term equal to the corresponding dark counting rate. We shall not consider these effects since we assume that all the intrinsic excitations occur within the sensor.

III. EXPERIMENTS AND QJS ENGINEERING

Now we shall compare the predictions of our model with the available experimental data. Experimentally, the dependences of both bright and dark counting rates are set as functions of the wavelength of the light and the 'bias parameter' (BP) of the detector. By BP we englobe such quantities as bias voltage, bias current or any other physical parameter the experimentalist adjusts in order to achieve simultaneously the best Signal-to-Noise ratio $\mathcal{S}$ and the highest bright counting rate. $\mathcal{S}$ is the ratio between the bright counting rate $\mathcal{R}_B$ and the dark one $\mathcal{R}_D$, $\mathcal{S} \equiv \mathcal{R}_B/\mathcal{R}_D$, and it has the following useful property: as one increases the value of BP, the bright counting rates increases while the $\mathcal{S}$ remains the same until the *breakdown* value of BP, after which the $\mathcal{S}$ starts to fall rapidly as function of BP. So most detectors usually

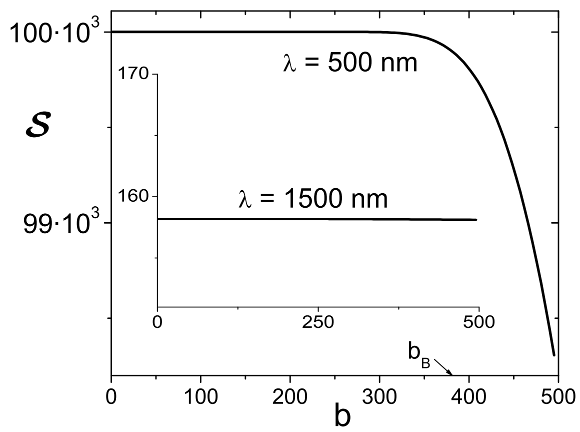

FIG. 1: Signal-to-Noise ratio as function of b at resonance ($\lambda = 500$ nm) and far from it ($\lambda = 1500$ nm) in the inset. The estimated breakdown value is $b_B \simeq 380$.

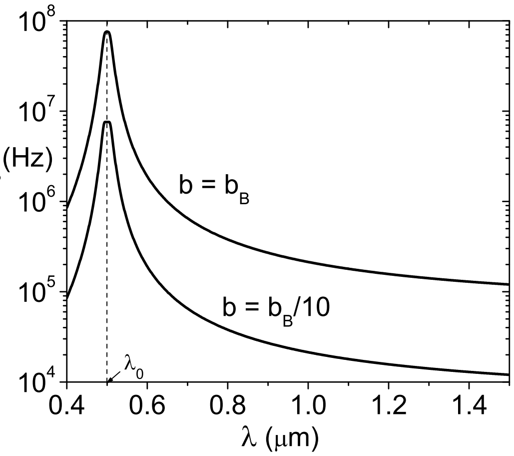

FIG. 2: Bright counting rate as function as wavelength of the field for different values of b, showing that $\mathcal{R}_B$ increases proportionally to b. The resonant wavelength is $\lambda_0 = 500$ nm.

operate near the breakdown BP in order to achieve the optimal performance. Experimentally [4], $\mathcal{R}_B$ is determined by directing laser pulses containing single photons at a given repetition rate on the detector and calculating the rate of counts, so in our model it is described by the term $J_1^{(B)}$; analogously, $\mathcal{R}_D$ is calculated in the absence of any input signal, so it is given by $J_0^{(D)}$.

To do the comparison with experimental results first we need to set the values of our model free parameters: ω_0, g, τ and $\bar{n}$; for the sake of better comparison we shall express the frequencies ω_0 and ω in terms of respective wavelengths λ_0 and λ. Thus we are left with only two experimental variables: λ and b, where b plays the role of BP. Meanwhile, our general model can't take into account the BP $\times$ b dependence for every kind of detector; nevertheless, one can argue that BP and b must be proportional to each other, since for zero BP one should also have $b = 0$, since in this case the detector would be turned off. Fortunately, we do not need to know the exact dependence of BP on b provided we determine the breakdown value b_B corresponding to the breakdown BP at the resonance and take it as a measure of b. So b_B will be our last fixed parameter, even though dependent on the free parameters, needed to compare the model predictions with experiment.

After several numerical simulations we have chosen the following values for our model free parameters that reproduce qualitatively the common experimental behavior [3, 4, 5, 6] and lie within the applicability region of the Jaynes–Cummings Hamiltonian (3) and the master equation (4): $\lambda_0 = 500$ nm, $g = 10^{11}$ Hz, $\tau = 5 \times 10^5$ and $\bar{n} = 10^{-11}$, so $b_B \simeq 380$, as shown in figure 1. Notice that 1) the values of $\mathcal{S} \simeq 10^5$ at the resonance ($\lambda = 500$ nm, $q = 0$) and 10^2 'far away' from it ($\lambda = 1.5$ μm, $q \gg 1$) are quite realistic, and 2) the chosen mean number of intrinsic excitations $\bar{n}$ is much larger than the number of thermal photons as calculated from Planck's distribution for room temperature ($\bar{n}_P \simeq 10^{-30}$), meaning that the contribution from defects within the detector is much stronger than the one from thermal photons (remember that we are considering a specific part of dark counts, as described in section II). Moreover, we verified that below b_B both $\mathcal{R}_B$ and $\mathcal{R}_D$ depend approximately linearly on b, which is in agreement with our qualitative arguments.

In figure 2 we have a plot of the $\mathcal{R}_B$ for two different values of b as function of the field wavelength, which shows a good agreement, qualitatively and quantitatively, with experimental results and illustrates the fact that $\mathcal{R}_B$ increases proportionally to b. We could confirm numerically that $\mathcal{R}_D$ does not depend on the field wavelength as expected, because the dark counts are detector's internal events.

So our model agrees qualitatively in all aspects with the experimental data. Now we turn to our main goal: how the QJS depends on the experimental detector parameters? First, we check that for the chosen parameters the *emission terms* ($J_n^{(E)}$ and further terms in Eq. (29)) *are at least 10 orders of magnitude smaller than the dark counts term and even more for bright counts term*, which confirms that detectors indeed do not emit photons into the field. Intuitively, the photon emissions by the detector would be possible only at temperatures much higher than room temperature through black body radiation, which is not the case in experiments.

Thus, in practice one is dealing only with bright and dark counts terms that act on the field simultaneously every time a count is registered, so the QJS has the fol-

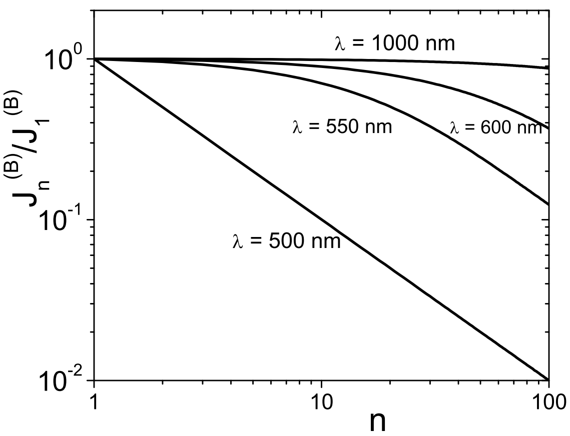

FIG. 3: Normalized bright counts term as function of n in di-log scale at breakdown b_B for different field wavelengths. At resonance ($\lambda = 500$ nm) we have $\beta \simeq 1/2$ and far away from resonance ($\lambda = 1000$ nm) $\beta \simeq 0$.

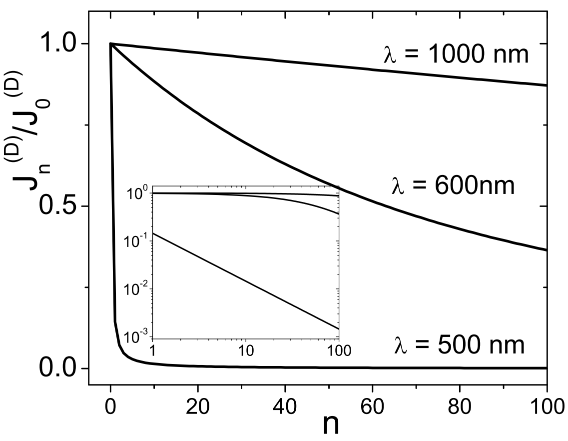

FIG. 4: Normalized dark counts term as function of n at breakdown b_B for different field wavelengths and the same graph in di-log scale in the inset.

lowing (diagonal) form in Fock basis

$$\hat{J}\rho = \text{diag}\left[\left(\hat{J}_B + \hat{J}_D\right)\rho\right]. \tag{35}$$

In figure 3 we show the dependence of the normalized bright counts term $J_n^{(B)}/J_1^{(B)}$ on n in di-log scale (for better visualization we joined the points). We note that near and far away from resonance one has nearly polynomial dependence (linear in di-log scale)

$$J_n^{(B)} \approx J_1^{(B)} n^{-2\beta} = \mathcal{R}_B \; n^{-2\beta} \tag{36}$$

with $\beta \simeq 1/2$ at resonance and $\beta \simeq 0$ far away from it. Thus, in these cases one can write the operator dependence of bright counts term as

$$\hat{J}_B\rho = \mathcal{R}_B \; (\hat{n}+1)^{-\beta} \, \hat{a}\rho\hat{a}^\dagger \, (\hat{n}+1)^{-\beta}, \tag{37}$$

thus recovering the E-model with $\beta \simeq 1/2$ at the resonance and SD-model with $\beta \simeq 0$ far away from it ($\lambda = 1$ μm). This is an important result: by just modifying the wavelength of the field one can engineer the QJS, obtaining one of the *ad hoc* proposals or another.

Now we turn to the normalized dark counts term $J_n^{(D)}/J_0^{(D)}$, shown in figure 4 in linear scale and in di-log scale in the inset. First, we see that out of resonance ($\lambda = 1$ μm) $J_n^{(D)}$ is almost independent on n, so we can set in this case $J_n^{(D)} \approx \mathcal{R}_D = \text{const}$. At resonance ($\lambda = 500$ nm), we see that for $n = 0$ one gets $J_0^{(D)} = \mathcal{R}_D$ and for $n > 0$ we have $J_{n>0}^{(D)} \approx d \cdot \mathcal{R}_D \cdot n^{-2\beta}$, where $\beta \simeq 1/2$ and d is a number less than 1. This means that at resonance the dark counts are suppressed by the presence of light, being generated predominantly by vacuum fluctuations. This can be understood by the following argument: the dark counts occur when the detector, in the ground state, is intrinsically excited by its excitations; but at resonance, the rate of excitations by field photons is much greater than the one by the intrinsic excitations, so the dark counts 'have no time' to appear and therefore become suppressed. Thus, the operator form of the dark counts term in Eq. (29) is

$$\hat{J}_D\rho = \mathcal{R}_D\left[\Lambda_0\rho\Lambda_0 + d\Lambda\hat{n}^{-\beta}\rho\hat{n}^{-\beta}\Lambda\right], \tag{38}$$

where $\Lambda_0 \equiv |0\rangle\langle 0|$, $\Lambda \equiv 1 - \Lambda_0$ and at resonance we have E-model with $\beta \simeq 1/2$ and $d < 1$. Far away from the resonance we recover the SD-model with $\beta \simeq 0$ and $d = 1$. Thus by operating near breakdown BP and by varying the wavelength of the field one can engineer the QJS and predict its bright and dark counts terms behavior; the only inconvenience for obtaining SD-model is that the $\mathcal{S}$ ratio is smaller than for E-model, since in this case one should operate far away from the resonance. For the sake of completeness we could also add to the right-hand side of Eq. (38) a constant term ($\mathcal{R}_D{}'\rho$) for the dark counts that do not cause the transition $|g\rangle \rightarrow |e\rangle$ inside the sensor, however the present model does not embraces such phenomena.

IV. SUMMARY AND CONCLUSIONS

We presented a microscopic model for a realistic photodetector in which we modelled it as a 2-level quantum sensor plus a macroscopic amplification mechanism. Using the quantum trajectories approach we deduced a general QJS describing the back-action of the detector on the field upon a photocount and showed that it

can be represented formally as an infinite sum of terms. In that sum we have identified the terms corresponding to the bright counts (real photoabsorptions), the dark counts and emission events, each one occurring with its respective probability. Adjusting the free parameters of the model to fit experimental data, we showed that the emission terms can be disregarded in realistic situations since their contribution becomes insignificant, so the QJS consists effectively only of bright and dark counts terms. Moreover, we reproduced qualitatively and quantitatively the experimental behavior of the counting rates and the Signal-to-Noise ratio, showing the breakdown phenomenon. Finally, we showed that with the detector operating near its breakdown bias one can engineer the QJS by modifying the wavelength of the field. In particular, one recovers the QJS's proposed previously *ad hoc*: at resonance one gets the E-model, and far away from it the SD-model is identified. Last but not least, the contribution of the dark counts to the QJS was derived within the context of a photocount model.

Acknowledgments

Work supported by FAPESP (SP, Brazil) contract # 04/13705-3. SSM and VVD acknowledge partial financial support from CNPq (DF, Brazil). We would like to thank the anonymous referees for valuable suggestions.

[1] A. Migdall and J. Dowling (eds.), Special issue of J. Mod. Opt. **51**, no. 9-10 (2004).
[2] S. Komiyama, O. Astafiev, V. Antonov, T. Kutsuwa, and H. Hirai, Nature **403**, 405 (2000).
[3] A. Rochas, M. Gani, B. Furrer, P. A. Besse, R. S. Popovic, G. Ribordy, and N. Gisin, Rev. Sci. Instr. **74**, 3263 (2003).
[4] A. Verevkin et al., Appl. Phys. Lett. **80**, 4687 (2002).
[5] J. Kitaygorsky et al., IEEE Trans. Appl. Superconductivity **15**, 545 (2005).
[6] A. Korneev et al., Appl. Phys. Lett. **84**, 5338 (2004).
[7] P. G. Kwiat, A. M. Steinberg, R. Y. Chiao, P. H. Eberhard, and M. D. Petroff, Phys. Rev. A **48**, R867 (1993).
[8] A. Karlsson, M. Bourennane, G. Ribordy, H. Zbinden, J. Brendel, J. Rarity, and P. Tapster, IEEE Circuits and Devices Mag. **15** (6), 34 (1999).
[9] A. J. Miller, S. W. Nam, J. M. Martinis, and A. V. Sergienko, Appl. Phys. Lett. **83**, 791 (2003).
[10] S. Takeuchi, J. Kim, Y. Yamamoto, and H. H. Hogue, Appl. Phys. Lett. **74**, 1063 (1999).
[11] A. Korneev et al., Microelectronic Engineering **69**, 274 (2003).
[12] G. Karve et al., Appl. Phys. Lett. **86**, 063505 (2005).
[13] M. D. Srinivas and E. B. Davies, Opt. Acta **28**, 981 (1981); **29**, 235 (1982).
[14] G. J. Milburn and D. F. Walls, Phys. Rev. A **30**, 56 (1984); H. M. Wiseman and G. J. Milburn, *ibid.* **47**, 642 (1993); G. S. Agarwal, M. Graf, M. Orszag, M. O. Scully, and H. Walther, *ibid.* **49**, 4077 (1994); J. Calsamiglia, S. M. Barnett, N. Lütkenhaus, and K-A. Suominen, *ibid.* **64**, 043814 (2001); G. A. Prataviera and M. C. de Oliveira, *ibid.* **70**, 011602(R) (2004).
[15] M. C. de Oliveira, L. F. da Silva, and S. S. Mizrahi, Phys. Rev. A **65**, 062314 (2002).
[16] H. Saito and M. Ueda, Phys. Rev. A **68**, 043820 (2003).
[17] M. Ueda, N. Imoto, and T. Ogawa, Phys. Rev. A **41**, 3891 (1990); M. Ueda, N. Imoto, and H. Nagaoka, *ibid.* **53**, 3808 (1996).
[18] A. V. Dodonov, S. S. Mizrahi, and V. V. Dodonov, J. Opt. B: Quantum Semiclassical Opt. **7**, 99 (2005).
[19] M. Ueda, N. Imoto, and T. Ogawa, Phys. Rev. A **41**, 6331 (1990).
[20] M. Ban, Phys. Rev. A **51**, 1604 (1995).
[21] C. T. Lee, Phys. Rev. A **48**, 2285 (1993); **49**, R633 (1994).
[22] A. V. Dodonov, S. S. Mizrahi and V. V. Dodonov, Phys. Rev. A **75**, 013806 (2007).
[23] L.-M. Duan, M. D. Lukin, J. I. Cirac, and P. Zoller, Nature **414**, 413 (2001).
[24] M. G. A. Paris, Phys. Lett. A **289**, 167 (2001).
[25] A. Miranowicz, J. Opt. B: Quantum Semiclass. Opt. **7**, 142 (2005).
[26] J.-C. Boileau, J. Batuwantudawe, and R. Laflamme, Phys. Rev. A **72**, 032321 (2005).
[27] C. Invernizzi, S. Olivares, M. G. A. Paris, and K. Banaszek, Phys. Rev. A **72**, 042105 (2005).
[28] S. Panda, B. K. Panda, and S. G. Mishra, Phys. Rev. B **69**, 195304 (2004).
[29] P. Warszawski and H. M. Wiseman, J. Opt. B: Quantum Semiclass. Opt. **5**, 1, 15 (2002).
[30] Y. Kang, H. X. Lu, Y.-H. Lo, D. S. Bethune, and W. P. Risk, Appl. Phys. Lett. **83**, 2955 (2003).
[31] Y. Ben-Aryeh and C. Brif, e-print quant-ph/9504009.
[32] M. C. de Oliveira, S. S. Mizrahi, and V. V. Dodonov, J. Opt. B: Quantum Semiclassical Opt. **5**, S271 (2003).
[33] A. V. Dodonov, S. S. Mizrahi, and V. V. Dodonov, Phys. Rev. A **72**, 023816 (2005).
[34] P. Warszawski, H. M. Wiseman, and H. Mabuchi, Phys. Rev. A **65**, 023802 (2002).
[35] P. P. Rohde and T. C. Ralph, J. Mod. Opt. **53**, 1589 (2006).
[36] E. T. Jaynes and F. W. Cummings, Proc. IEEE **51**, 89 (1963).
[37] A. B. Klimov, I. Sainz, and S. M. Chumakov, Phys. Rev. A **68**, 063811 (2003).
[38] M. D. Crisp, Phys. Rev. A **43**, 2430 (1991).
[39] H. Carmichael, *An Open Systems Approach to Quantum Optics* (Springer, Berlin, 1993).
[40] S. Stenholm, Phys. Rep. **6**, 1 (1973).
[41] J. D. Cresser and S. M. Pickles, Quantum Semiclassical Opt. **8**, 73 (1996).